

## Metal-Ion Enhanced Helicity in the Gas Phase

Motoya Kohtani, Brian S. Kinnear, and Martin F. Jarrold\*

Department of Chemistry, Northwestern University  
2145 Sheridan Road, Evanston, Illinois 60208

Received July 10, 2000

Recent studies have shown that protonated polyaniline peptides  $(Ala_n+H)^+$  are not helical in the gas phase,<sup>1,2</sup> despite alanine's high helix propensity in solution.<sup>3</sup> Here we show that substituting an alkali metal ion ( $Li^+$ ,  $Na^+$ ,  $K^+$ ,  $Rb^+$ , or  $Cs^+$ ) for the proton leads to a transformation from a random globule to a rigid helix. While metal ions have been found to enhance the helicity of small peptides in aqueous solution,<sup>4–8</sup> this often involves residues with high metal affinities locking in the helical conformation by formation of metal-mediated cross-links. The peptides discussed here do not have metal-complexing side chains. The enhanced helicity apparently results because the oxyphilic metal ions coordinate to CO groups at the C-terminus. This "caps" the helix<sup>9,10</sup> and allows favorable interactions between the metal ion and the helix dipole.<sup>11–13</sup>

The interactions between metal ions and proteins play many important roles in energy metabolism and signaling. Metal ions often cause conformational changes when they bind to proteins, which can profoundly affect their properties.<sup>14–17</sup> Metal ion interactions also provide a valuable tool in the design of proteins.<sup>18–21</sup> There have been a number of experimental and theoretical studies of the interactions between small peptides and metal ions in the gas phase. These studies have focused on the energetics and location of metal binding,<sup>22–25</sup> on the conformations

of metal ion–peptide complexes,<sup>26,27</sup> on whether metal ions can stabilize zwitterions in small peptides,<sup>28–30</sup> and on possible applications of metal ions in sequencing.<sup>31</sup>

In the work reported here we have used high-resolution ion mobility measurements<sup>32</sup> to probe the conformations of  $(Ala_n+M)^+$  peptides with  $M = Li, Na, K, Rb,$  and  $Cs$  and  $n = 6–20$ . The mobility, how rapidly an ion moves through a buffer gas under the influence of a weak electric field, depends on the average collision cross section, which in turn depends on the conformation.<sup>33–36</sup> The high-resolution ion mobility apparatus consists of an electrospray source, a 63 cm long drift tube, a quadrupole mass spectrometer, and a detector.<sup>32,37</sup> Solutions were prepared by dissolving 1 mg of peptide in 1 mL of TFA and 0.1 mL of water. The appropriate chloride salt was then added to bring the metal ion concentration to approximately  $10^{-2}$  M. Figure 1 shows relative cross sections (derived from the measured drift times<sup>38</sup>) for  $(Ala_n+M)^+$ ,  $M = Li, Na, K, Rb,$  and  $Cs$ , and  $(Ala_n+H)^+$ <sup>1</sup> plotted against the number of residues. The relative cross section scale is given by  $\Omega_{rel} = \Omega_{meas} - 14.50n$  where  $\Omega_{meas}$  is the measured average cross section,  $n$  is the number of residues, and  $14.50 \text{ \AA}^2$  is the increment per residue in the calculated cross section for an ideal polyaniline  $\alpha$ -helix. With this scale, the relative cross sections of  $\alpha$ -helices are independent of the number of residues, while the more compact random globule conformations have values that decrease with increasing peptide size. The cross sections for the  $(Ala_n+H)^+$  peptides show this behavior. On the other hand, the results for  $(Ala_n+M)^+$ ,  $M = Li, Na, K, Rb,$  and  $Cs$  are largely independent of  $n$ , which is characteristic of helical conformations. For small peptides, the helix and globule have similar cross sections. It will become apparent from simulations described below that we can safely conclude that  $(Ala_n+M)^+$  peptides with  $M = Li, Na, K, Rb,$  and  $Cs$  are helical for  $n > 12$ . Smaller peptides (except perhaps for  $M = Li$ ) may also be helical, but the cross sections are not sensitive enough to distinguish the helix and globule definitively.

It has been suggested that the  $(Ala_n+H)^+$  peptides are not helical because protonation at the N terminus (the most basic site) leads to unfavorable interactions with the helix dipole.<sup>36,39</sup> Thus, for the metalated polyaniline peptides to become helical the metal ion should probably be located at the C terminus. To provide more insight into the binding of the metal ion, molecular dynamics (MD) simulations were performed for  $(Ala_n+Na)^+$  with  $n = 10, 15,$  and  $20$ . The simulations were performed using the MACSI-

(1) Hudgins, R. R.; Mao, Y.; Ratner, M. A.; Jarrold, M. F. *Biophys. J.* **1999**, *76*, 1591–1597.

(2) Samuelson, S.; Martyna, G. J. *J. Phys. Chem. B* **1999**, *103*, 1752–1766.

(3) Chakrabarty, A.; Baldwin, R. L. *Adv. Protein Chem.* **1995**, *46*, 141–176.

(4) Ghadiri, M. R.; Choi, C. J. *Am. Chem. Soc.* **1990**, *112*, 1630–1632.

(5) Ruan, F.; Chen, Y.; Hopkins, P. B. *J. Am. Chem. Soc.* **1990**, *112*, 9403–9404.

(6) Impellizzeri, G.; Pappalardo, G.; Purrello, R.; Rizzarelli, E.; Santoro, A. M. *Chem. Eur. J.* **1998**, *4*, 1791–1798.

(7) Siedlecka, M.; Goch, G.; Ejchart, A.; Sticht, H.; Bierzynski, A. *Proc. Natl. Acad. Sci. U.S.A.* **1999**, *96*, 903–908.

(8) Hémin, O.; Barbier, B.; Boillot, F.; Brack, A. *Chem. Eur. J.* **1999**, *5*, 218–226.

(9) Forood, B.; Feliciano, E. J.; Nambiar, K. P. *Proc. Natl. Acad. Sci. U.S.A.* **1993**, *90*, 838–842.

(10) Presta, L. G.; Rose, G. D. *Science* **1988**, *240*, 1632–1641.

(11) Daggett, V. D.; Kollman, P. A.; Kuntz, I. D. *Chem. Scr.* **1989**, *29A*, 205–215.

(12) Blagdon, D. E.; Goodman, M. *Biopolymers* **1975**, *14*, 241–245.

(13) Seale, J. W.; Srinivasan, R.; Rose, G. D. *Protein Sci.* **1994**, *3*, 1741–1745.

(14) Ogut, O.; Jin, J.-P. *Biochemistry* **1996**, *35*, 16581–16590.

(15) Asante-Appiah, A.; Skalka, A. M. *J. Biol. Chem.* **1997**, *272*, 16196–16205.

(16) Ippolito, J. A.; Steitz, T. A. *Proc. Natl. Acad. Sci. U.S.A.* **1998**, *95*, 9819–9824.

(17) Stout, J. G.; Zhou, Q.; Wiedmer, T.; Sims, P. J. *Biochemistry* **1998**, *37*, 14860–14866.

(18) Schneider, J. P.; Kelly, J. W. *J. Am. Chem. Soc.* **1995**, *117*, 2533–2546.

(19) Cheng, R. P.; Fisher, S. L.; Imperiali, B. *J. Am. Chem. Soc.* **1996**, *118*, 11349–11356.

(20) Kohn, W. D.; Kay, C. M.; Sykes, B. D.; Hodges, R. S. *J. Am. Chem. Soc.* **1998**, *120*, 1124–1132.

(21) Suzuki, K.; Hiroaki, H.; Kohda, D.; Nakamura, H.; Tanaka, T. *J. Am. Chem. Soc.* **1998**, *120*, 13008–13015.

(22) Klassen, J. S.; Anderson, S. G.; Blades, A. T.; Kebarle, P. *J. Phys. Chem.* **1996**, *100*, 14218–14227.

(23) Cerda, B. A.; Hoyau, S.; Ohanessian, G.; Wesdemiotis, C. *J. Am. Chem. Soc.* **1998**, *120*, 2437–2448.

(24) Ohanessian, G.; Hoyau, S. *Chem. Eur. J.* **1998**, *4*, 1561–1569.

(25) Shields, S. J.; Bluhm, B. K.; Russell, D. H. *J. Am. Soc. Mass Spectrom.* **2000**, *11*, 626–638.

(26) Taraszka, J. A.; Li, J.; Clemmer, D. E. *J. Phys. Chem. B* **2000**, *104*, 4545–4551.

(27) Taraszka, J. A.; Counterman, A. E.; Clemmer, D. E. Large Anhydrous Polyaniline Ions: Substitution of  $Na^+$  for  $H^+$  Destabilizes Folded States. *Int. J. Mass Spectrom.* Manuscript submitted.

(28) Wyttenbach, T.; Bushnell, J. E.; Bowers, M. T. *J. Am. Chem. Soc.* **1998**, *120*, 5098–5103.

(29) Wyttenbach, T.; Witt, M.; Bowers, M. T. *J. Am. Chem. Soc.* **2000**, *122*, 3458–3464.

(30) Jockusch, R. A.; Price, W. D.; Williams, E. R. *J. Phys. Chem. A* **1999**, *103*, 9266–9274.

(31) Lee, S.-W.; Kim, H. S.; Beauchamp, J. L. *J. Am. Chem. Soc.* **1998**, *120*, 3188–3195.

(32) Dugourd, Ph.; Hudgins, R. R.; Clemmer, D. E.; Jarrold, M. F. *Rev. Sci. Instrum.* **1997**, *68*, 1122–1129.

(33) Hagen, D. F. *Anal. Chem.* **1979**, *51*, 870–874.

(34) Von Helden, G.; Hsu, M.-T.; Kemper, P. R.; Bowers, M. T. *J. Chem. Phys.* **1991**, *95*, 3835–3837.

(35) Clemmer, D. E.; Jarrold, M. F. *J. Mass Spectrom.* **1997**, *32*, 577–592.

(36) Hudgins, R. R.; Ratner, M. A.; Jarrold, M. F. *J. Am. Chem. Soc.* **1998**, *120*, 12974–12975.

(37) Hudgins, R. R.; Woenckhaus, J.; Jarrold, M. F. *Int. J. Mass. Spectrom. Ion Processes* **1997**, *165/166*, 497–507.

(38) Mason, E. A.; McDaniel, E. W. *Transport Properties of Ions in Gases*; Wiley: New York, 1988.

(39) Hudgins, R. R.; Jarrold, M. F. *J. Am. Chem. Soc.* **1999**, *121*, 3494–3501.

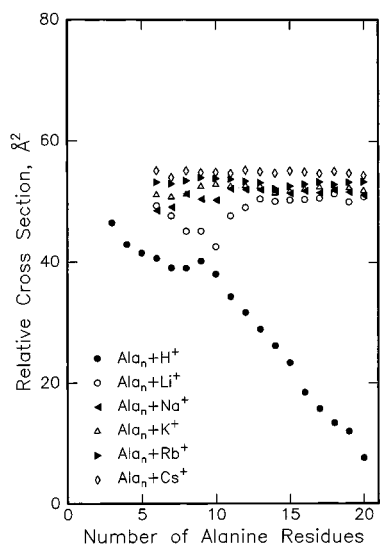


**Figure 1.** Relative cross sections plotted against number of alanine residues for  $(Ala_n+H)^+$  and  $(Ala_n+M)^+$  with  $M = Li, Na, K, Rb,$  and  $Cs$ . Relative cross sections that are independent of the number of residues indicate helical conformations, while relative cross sections that decrease with increasing peptide size (like those for the  $(Ala_n+H)^+$  peptides) indicate random globules.

MUS suite of programs<sup>40</sup> with CHARMM-like potentials (21.3 parameter set).<sup>41</sup> Multiple simulated annealing runs were performed for  $n = 15$  and  $20$  (starting from a helix) in an effort to identify the preferred binding geometry. We found that the  $Na^+$  ion always migrated to the C terminus (even when initially placed near the middle of the helix). At the C terminus the sodium ion coordinates to several carbonyl groups.  $Na^+$  is oxyphilic, so that a preference for binding to carbonyl groups is expected.<sup>23</sup> The extent to which the C terminus is disrupted by the  $Na^+$  ion varies significantly. Figure 2(a) shows the final conformation from the  $(Ala_{20}+Na)^+$  simulated annealing run with the lowest terminal energy. Here the  $Na^+$  ion is coordinated to the carboxyl CO and backbone CO groups of residues 15, 16, 17, and 19. Virtually the entire helix remains intact. In this geometry there are favorable charge-dipole interactions and the  $Na^+$  “caps” several of the dangling CO groups at the C terminus. This type of conformation occurred frequently. Figure 2b shows another type of conformation that occurred often. Here the C terminus is slightly more unraveled and wraps around the  $Na^+$ . In this particular geometry, the  $Na^+$  is coordinated to the carboxyl CO and backbone CO groups of residues 12, 13, 15, and 17. This conformation is  $8 \text{ kJ mol}^{-1}$  less stable than the one shown in Figure 2a, a difference which cannot be viewed as significant. Average cross sections<sup>42</sup> calculated from the last 60 ps of the simulations leading to the conformations in Figure 2a and b are both in good agreement with the measured value. The Boltzmann weighted average cross section for all of the  $(Ala_{20}+Na)^+$  simulations is  $341.6 \text{ \AA}^2$  which can be compared with the measured value of  $340.7 \text{ \AA}^2$ . For  $(Ala_{15}+Na)^+$  the Boltzmann weighted average and measured values are  $266.5$  and  $268.6 \text{ \AA}^2$ , respectively. The good agreement between the measured and calculated cross sections provides a strong indication that the ions adopt the largely helical conformations shown in Figure 2a and b. A few simulated annealing runs led to conformations where the helix is significantly more unraveled. An example is shown in Figure 2c. The more unraveled conformations are significantly less stable than the more helical ones (by  $59 \text{ kJ mol}^{-1}$  for the geometry in Figure 2), and their

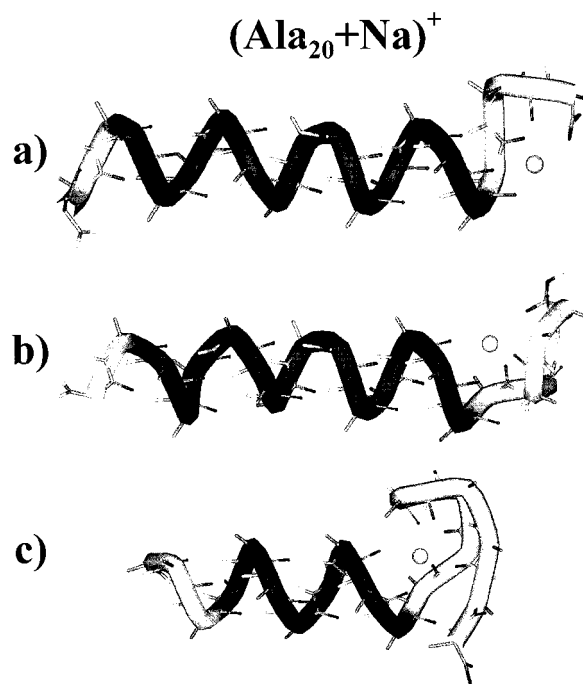


**Figure 2.** Final conformations from simulated annealing runs for  $(Ala_{20}+Na)^+$ ; (a) and (b) have approximately the same energies and both have calculated cross sections that are close to the measured value; (c) is significantly higher in energy, and its calculated cross section is substantially less than the measured value.

calculated average cross sections are substantially smaller than the measured value.

For  $(Ala_{10}+Na)^+$  most of the simulated annealing runs collapsed into random globules, while room temperature MD simulations (240 ps) started from a helix usually remained helical. The resulting helices and globules have similar energies (the lowest-energy helix found is  $9 \text{ kJ mol}^{-1}$  lower than the lowest-energy globule). The measured cross section ( $195.0 \text{ \AA}^2$ ) is in slightly better agreement with the value calculated for the helices ( $194.6 \text{ \AA}^2$ ) than for the globules ( $189.2 \text{ \AA}^2$ ). The small difference between the calculated cross sections for the helix and globule prevents a definitive statement, but  $(Ala_{10}+Na)^+$  is probably largely helical (the accepted error margin for comparison of measured and calculated cross sections is 2%). The similarity between the results for the different  $(Ala_n+M)^+$  ions suggests that complexes of  $Ala_{10}$  with  $K^+$ ,  $Rb^+$ , and  $Cs^+$  are also largely helical.  $Li^+$  may be the exception. The small relative cross section for  $(Ala_{10}+Li)^+$  may indicate a globular conformation. This provides better self-solvation for the  $Li^+$  ion (which is smaller and has a higher charge density than the other alkali metals).

Metal ions have recently been shown to stabilize zwitterions in small peptides.<sup>28–30</sup> In simulations, helical  $(Ala_{15}+Na)^+$  zwitterions with the N terminus protonated and the C terminus deprotonated rapidly collapse to random globules (the charge destabilizes the helix). A helix with a salt bridge from deprotonation of the C terminus and protonation of the backbone (CO) near to the C terminus appears to be stable in the simulations. However, formation of this salt bridge seems unlikely because the backbone is not very basic. Cross sections measured for amidated  $(Ala_n-NH_2+Na)^+$  peptides (where salt bridge formation is blocked at the C terminus) track those measured for the  $(Ala_n+Na)^+$  peptides, and thus the enhanced helicity observed with the metal ions does not result from salt bridge formation.

**Acknowledgment.** We thank Jiri Kolafa for use of his MACSIMUS molecular modeling programs, and for his helpful advice. We gratefully acknowledge the support of the National Institutes of Health.

JA002485X

(40) Kolafa, J. <http://www.icpf.cas.cz/jiri/macsimus/default.htm>.

(41) Brooks, B. R.; Bruccoleri, R. E.; Olafson, B. D.; States, D. J.; Swaminathan, S.; Karplus, M. *J. Comput. Chem.* **1983**, *4*, 187–217.

(42) The cross sections were calculated by the trajectory method described in Mesleh, M. F.; Hunter, J. M.; Shvartsburg, A. A.; Schatz, G. C.; Jarrold, M. F. *J. Phys. Chem.* **1996**, *100*, 16082–16086.